An evaluation of potential materials for the handling and support of mass standards in vacuum/inert gas apparatus

James Berry[1], Stuart Davidson, Stephen Downes[1], Richard Högström[2], Zaccaria Silvestri[3]

[1]National Physical Laboratory, Hampton Road, Teddington, Middlesex, TW11 0LW, UK
[2]Mittatekniikan Keskus, PL9, Tekniikantie 1, 02151 Espoo, Finland
[3]Laboratoire commun de métrologie, Conservatoire national des arts et métiers, 61 rue du Landy, F-93210, La Plaine Saint-Denis.

Abstract

This paper reports on research undertaken to evaluate the suitability of potential materials for the handling and support of mass standards in vacuum / inert gas apparatus. Primary mass standards are currently stored in air at atmospheric pressure and the chamois leather and tissue paper used to support and handle them are not compatible with use in a vacuum. Aluminium, titanium, polytetrafluoroethylene, polyether ether ketone and polyamide-imide materials were selected as potential materials suitable for use in a vacuum / inert gas environment. The suitability of these materials was evaluated by assessing the thermal desorption properties of the polymeric materials and assessing the effect that all of the materials have on the surface of stainless steel artefacts through repeated contact.

All of the materials were found to mark the stainless steel artefacts through contact. Polyether ether ketone, aluminium and polyamide-imide did similar amounts of damage to the surface. The results from the Mittatekniikan Keskus laboratory showed that the polytetrafluoroethylene material caused the least amount of damage but did transfer some material to the surface. However, this was in contrast with the data obtained by the National Physical Laboratory which showed that the polytetrafluoroethylene did similar levels of damage as the other polymer materials. The titanium material appeared to cause the next least amount of damage and did not transfer any significant amount of material. The results of the thermal desorption measurements showed that polyamide-imide desorbed much higher levels of water in vacuum compared with both polytetrafluoroethylene and polyether ether ketone.

1 Background

The current definition of the SI unit of mass is defined in terms of a physical artefact manufactured from an alloy of platinum-iridium (Pt-Ir), namely the international prototype of the kilogram [1]. Experiments are underway to redefine the SI unit of mass in terms of a fundamental physical constant of nature [2, 3]. However, physical mass artefacts will remain necessary for providing traceability from a new primary realisation in a vacuum environment to secondary standards at atmospheric air pressures. Furthermore, these mass artefacts will need to be transported between primary realisation experiments at different national laboratories and stored between measurements in a way that minimises surface contamination forming on them.

Current methods of supporting prototype kilogram artefacts during storage or transport typically involve the use of a clamping mechanism covered with a layer of chamois leather and then a top layer of either lens tissue paper or acid free tissue paper [4]. This method is appropriate for supporting mass artefacts in air, though it is not suitable for supporting mass artefacts in vacuum due to the likelihood of outgassing of hydrocarbon contaminants from the chamois leather or tissue paper during vacuum exposure which could deposit on the surface of a mass artefact. Both chamois leather and acid free tissue paper can also leave small fibres on the surface of mass artefacts which are easily removed from artefacts supported in air, using a small brush or jet of air, but would be more difficult to remove from artefacts supported in vacuum or inert gas. Previous work has researched the types of storage vessels and transfer equipment that are currently used to store and transport mass artefacts between realisation experiments and mass comparators [5]. Some research has been published which has examined the stability of weights during transport [6] and work by Davidson [7], Fuchs [8] and Berry [9] has examined the effect of different storage media on mass stability.

2 Introduction

The aim of the work described in this paper was to evaluate the suitability of a range of materials that could be used to support and handle mass artefacts during their storage and transportation between experiments to realise the kilogram and mass comparators. The ideal material would cause no damage to the surface of the mass artefact through repeated contact

or transfer any material to the surface of the artefact. Ideally the contact material would also have low outgassing rates when used in a vacuum.

This research was undertaken at three National Measurement Institutes (NMIs). Repetitive contact testing of five types of support material was performed at the National Physical Laboratory (NPL) and at the Mittatekniikan Keskus (MIKES). Research into the outgassing properties of the polymeric materials was undertaken at the Conservatoire national des arts et metiers (CNAM). Both NPL and MIKES modified the turntable of a commercial mass comparator with pegs manufactured from the chosen support materials and used the comparator mass handling mechanism to repeatedly apply the support materials to the test artefacts. Atomic force microscopy (AFM) and coherence scanning interferometry (CSI) were used to examine the surface of the test artefacts. CNAM used thermal desorption spectroscopy (TDS) to measure the rate of desorption of water, nitrogen and oxygen from the selected support materials as they were heated in a vacuum to 70 °C.

3 Support materials investigated

Five materials were investigated, namely polytetrafluoroethylene (PTFE), polyether ether ketone (PEEK), polyamide-imide (Torlon), aluminium, and titanium which are summarised in table 1. PTFE was selected as it is used to support mass artefacts in storage vessels by NPL, CNAM and Laboratoire National de Métrologie et d'Essais (LNE) [5], PEEK is used by the Bureau International des Poids et Mesures (BIPM) and Sartorius AG [5], Torlon has high wear resistance properties, and aluminium is commonly used in commercial mass comparators to support mass artefacts. The grade of PEEK tested by NPL was specified with 10 % carbon filler whilst CNAM tested two grades of PEEK; one without carbon filler, and one with 30 % carbon filler.

Table 1. Support materials investigated

Support Material	Specification
Aluminium	Alloy 6082 T6
PTFE	Tecaflon
PEEK	0 % carbon
PEEK	10 % carbon
PEEK	30 % carbon

Torlon	Grade 4435
Titanium	CAS 7440-32-6

4 Measurements at NPL

4.1 Test artefacts

Four cylindrical artefacts with diameters of 48 mm and depths of 12 mm were manufactured by Häfner (Germany) from HE210 stainless steel with a yield strength of 0.23 GPa. Häfner use the HE210 material to manufacture their class E0 mass standards. The surfaces of these artefacts were polished to have maximum roughness values that meet the criterion set by the International Organisation of Legal Metrology (OIML) [10] for E1 class weights which are 0.5 µm (R_z) and 0.1 µm (R_a). After polishing, the artefacts were cleaned using a two-stage process. The first cleaning stage comprised submersion of the artefacts in reagent grade ethanol (with a purity of at least 99.8%) in an ultrasonic bath for a period of 5 minutes. The second stage involved rinsing the artefacts with distilled water. A plastic squeeze bottle was used to produce a fine spray of distilled water that was directed across the surface of each artefact for about 5 minutes with the artefact rotated half way through this process to clean its bottom surface. Each artefact was allowed to dry in air with larger water droplets removed using clean lens tissue paper. The pegs were also cleaned by immersing them in ethanol in an ultrasonic bath for 5 minutes but they were not rinsed with distilled water afterwards and instead they were left to dry in air after removal from the ethanol.

4.2 Measurement apparatus

A Mettler-Toledo HK1000 mass comparator was used to repeatedly transfer the stainless steel artefacts onto the support materials. Three pegs of each support material were manufactured and inserted into holes machined into the comparator's turntable as shown in figure **Error! Reference source not found.**~~1~~. The holes were machined at 120° intervals on a circle with a radius of 30 mm. The vertical motion of the HK1000 turntable was controlled using software on a computer so that the entire test process was fully automated.

The surface topography of the stainless steel artefacts was determined with a CSI microscope (Wyko 9800) which was equipped with a white-light source. The diffraction-limited spatial

(*i.e.* lateral) resolution of this microscope can be estimated using the Rayleigh Criterion given by

$$r = 0.61\frac{\lambda}{N_{\mathrm{A}}}$$

where r is the least separation for resolution, λ the wavelength of the light used to illuminate a surface and N_{A} is the numerical aperture of the microscope's objective lens. Values of r for the microscope's 20× and 50× objective lenses are given in table 2 and have been calculated by assuming a value for λ of 525 nm which is the approximate mid-point of the microscope's white-light source.

Table 2. Estimation of the lateral resolution r of the Wyko 9800 microscope.

Objective	N_{A}	r /nm
20×	0.4	801
50×	0.6	534

In use, the actual resolution of the microscope is likely to be poorer than that predicted by the Rayleigh Criterion as aberrations in its optical system (e.g. imperfect lens geometry and alignment of the optical components) can also degrade the microscope's spatial resolution. The vertical resolution of this instrument has been measured and found to be generally less than 1 nm. In addition to the CSI measurements, an atomic force microscope (Park XE-100) was used in its non-contact mode to determine the surface topography of the artefact used with the aluminium test pegs.

4.3 Measurement procedure

The first artefact was loaded onto the turntable at the position equipped with the aluminium pegs and the comparator was used to lower the artefact to the weighing pan and then raise it again to its top position a total of ten thousand times. When the turntable was lowered to the weighing pan the artefact was lifted clear of the aluminium pegs and when the turntable was raised back to the top position the three pegs made contact with the bottom surface of the artefact and lifted it clear of the weighing pan. This measurement process was repeated using each of the three remaining artefacts contacting on the PTFE, PEEK and Torlon pegs

respectively. During all the contact tests the artefacts were seen to precess about a vertical axis that was at the approximate location of the midpoint of the three support pegs.

4.4 Results

4.4.1 Aluminium support tests

The surface of the artefact was damaged by its contact with the aluminium pegs and this damage occurred along arc profiles that correspond to the precession seen during the repeated contact tests. The structure of the damage generally had one of three forms: indentations (figure 2); indentations with material build-up (figure 3); and grooves (figure 4). The lateral dimensions of the indentations measured with the CSI microscope (figure 2) are approximately 2 μm with depths of around 15 nm to 20 nm. However, their topography seen with AFM (figure 6) reveals detail that the CSI instrument has not been able to resolve; whereas the CSI image shows the indentations as having a hemispherical form the AFM images reveal a more irregular shape that has lateral dimensions of approximately 500 nm and depths of around 100 nm. Comparison of these lateral dimensions with the estimated lateral resolution of the CSI microscope (table 2) shows the microscope will struggle to resolve these indentations. Furthermore, as the lateral resolution of an optical interferometric microscope is approached its amplitude transmission will fall [11,12] which leads to the microscope providing an underestimation of the vertical heights/depths of surface features. In the case for the indentations seen in figure 2, the CSI microscope has predicted depths which are only 20% of the values measured with AFM.

The indentations will be formed when the compressive stresses generated in the stainless steel exceed its local yield strength and their regular shapes imply the peg movement vector is normal to the artefact's surface. The manufacturers' values for the yield strengths of the stainless steel and aluminium are 0.23 GPa and 0.29 GPa respectively. This would suggest that the aluminium pegs are capable of causing the deformation directly. The irregular shape of these indentations (figure 6) however, suggests that a third-body might be involved in this process by becoming embedded in the aluminium peg.

Other regions on the stainless steel surface have indentations that appear elongated with material build-up next to the indentation. Figures 3 (CSI) and 7~~8~~ (AFM) give examples of this elongated structure (that have lateral dimensions of around 2 μm measured with AFM) which

implied there was an additional element of sliding contact between the peg and the artefact's surface. The depths of these indentations were typically around 300 nm which was a threefold increase compared to the indentations formed when there was only vertical loading of the peg. The grooves seen in figures 4 (CSI) and 5 (AFM) will have resulted from sliding contact between the aluminium peg and the artefact's surface and could have been created by a two-body wear mechanism or it is possible a third body (i.e. contamination) has been introduced from the surrounding environment. Finally, figure 8 is a CSI image of a region where significant damage has accrued on the artefact's surface through its repeated contact with the aluminium peg in the same nominal surface location (i.e. the artefact has stopped precessing).

4.4.2 PEEK, PTFE and Torlon support tests

The stainless steel surface has been damaged by its contact with the PEEK, PTFE and Torlon pegs. The form of the damage was similar for each of these materials and was either indentations with material build-up (*e.g.* figures 9, 11 ~~11~~ and 13) or grooves (*e.g.* figures 10, Figure 12~~12~~ and 14). The depths of the indentations and grooves appeared to be similar to those created by the aluminium pegs but these values may not be reliable as their lateral dimensions were similar to the resolution of the CSI instrument. In either case, the damage will have been caused by a three-body wear mechanism whereby the tips of the pegs have become contaminated from the surrounding environment with embedded particulates that have higher yield strength than the stainless steel.

5 Measurements at MIKES

5.1 Test artefacts

Stainless steel cylindrical artefacts with a diameter of 47 mm and nominal mass of 50 g were used for the contact experiments. These artefacts were manufactured by Häfner to the OIML E1 standard [10] and, as such, their material specifications and surface finish are equivalent to weights that are used as reference mass standards.

5.2 Measurement apparatus

Four different support materials were studied, namely PEEK, PTFE, aluminium, and titanium. The compatibility of the support materials with the stainless steel artefacts was studied by bringing the artefacts repeatedly into contact with the materials. A Sartorius C2000S mass comparator was programmed to repeatedly lower and raise the artefacts onto three support pegs manufactured from PEEK, PTFE, and titanium. The pegs were attached to the comparator turntable as shown in figure 15 and were evenly spaced to make contact near the perimeter of the artefact and ensure the forces acting on the artefact were similar at each contact point. The weighing pan of the mass comparator was made from aluminium and therefore it was not necessary to manufacture pins from this material.

The surface topography of the stainless steel artefacts has been determined using a PSIA XE-100 AFM. The optical microscope of the AFM was used to locate the contact areas on each artefact. These contact areas were easy to identify as the artefacts were observed to rotate during their repeated loading cycles which caused marks that followed the perimeter of each artefact. AFM topography images with dimensions of 50 µm × 50 µm and resolutions of 256 × 256 pixels were recorded at the contact areas. The AFM was operated in non-contact mode. Wear resistant cantilevers (Nanosensors PtSi-NCH) with typical spring constants of 42 N m^{-1}, tip radius of curvature 25 nm and resonant frequency of 330 kHz were used.

5.3 MIKES measurement procedure

The stainless steel artefacts were brought into contact with the support pegs at least 10 000 times. A different artefact was used for each set of support pegs and a weight with a nominal

mass of 500 g was placed on top of each artefact to simulate the forces encountered during weighing measurements made with real mass standards. At the end of each test the surface topography of the artefact was studied with the AFM.

5.4 Results

5.4.1 PEEK support tests

Repetitive contact between the stainless steel artefact and the pegs made of PEEK introduced clearly visible grooves following the perimeter of the artefact's surface. From the optical microscope image shown in figure 16 it can be seen that the grooves are formed from closely spaced identically shaped indentations. The depths of the indentations were measured using the AFM and the deepest ones were found to be about 300 nm deep as shown in figure 17. The damage observed in the optical microscope and AFM images was similar to that observed in the NPL PEEK support tests and was probably also caused by the same three-body wear mechanism (§ 4.4.2). Some contamination was observed near the indentations which was probably material that had disengaged from the PEEK pegs during contact.

5.4.2 Aluminium support tests

Grooves were observed on the stainless steel artefact after its repeated contact with the aluminium weighing pan and were similar to those observed after the PEEK support tests. Contact with the aluminium weighing pan has caused indentations on the surface that are visible in the optical microscope image shown in figure 18. These indentations appeared to be of a similar depth as those caused by PEEK contact. The shape of the indentations was, however, different and was probably due to the different shape of the weighing pan. Also, the damaged area was larger than for PEEK which was expected as the contact area of the weighing pan was larger than the PEEK pegs. AFM measurements gave a depth of about 200 nm for the indentations and a topography image from the AFM measurements is shown in figure 19. Moreover, very little or no excess contamination was found at the contact area. Again the damage observed in the optical microscope and AFM images was similar to that observed in the NPL support tests and was probably the result of the same wear mechanism (§ 4.4.1).

5.4.3 PTFE support tests

Contact with PTFE did not cause the type of groove observed with the PEEK and aluminium tests. However, the optical microscope images do show marks on the surface as seen in

figure 20. It can be seen from the AFM image shown in figure 21 that contact with the PTFE pegs did not caused indentations or depressions but there appeared to be considerable amount of contamination that had probably been transferred from the pegs. However, this contamination was negligible in terms of mass added to the artefact. These results were in contrast to the NPL PTFE contact tests which showed damage in the form of indentations on the surface of the artefacts in the CSI images (§ 4.4.2). The horizontal streaks observed in the AFM image shown in figure 21 were typical imaging artefacts and are not an indication of damage to the surface; these imaging artefacts may have arisen because the probe was unable to track sharp surface features as a result of improper feedback parameters.

5.4.4 Titanium support tests

Visual inspection of the stainless steel artefact after repeated contact with the titanium pegs has shown similar grooves generated during the PEEK tests. The optical microscope shows the indentations are smaller than those found in the PEEK studies as seen in the image in figure 22. The AFM measurements found the indentations to be much shallower than those observed in the PEEK measurements and have a depth of approximately 30 nm as shown in figure 23. The indentations were probably caused by the same wear mechanism as suggested for the aluminium pegs (§ 4.4.1) as the titanium material also had a yield strength (0.28 GPa) which was higher than the stainless steel material (0.23 GPa). Moreover, titanium contact introduced some surface contamination which is seen as white spots in the AFM image. The contamination was randomly distributed on the surface and thus was probably contaminant material originating from machining of the pegs that was transferred to the surface during contact.

6 CNAM Measurements

6.1 Measurement apparatus

Four discs were manufactured, each with a nominal diameter of 50 mm and thickness of 6 mm from PEEK 0% carbon, PEEK 30% carbon, PTFE and Torlon grade 4435 material. To achieve a good surface finish the discs were polished using SiC foil with a grit size of 4000 (supplied by Struers). The surface roughness values were measured using a portable surface tester (Mitutoyo SurfTest SJ-210) and table 3 gives typical roughness parameters (R_a, R_q and R_z) for each disc.

Table 3. Surface roughness parameters of the manufactured support material discs.

	PEEK 0%	PEEK 30%	PTFE	Torlon
R_a (µm)	0.08(0.01)	0.13(0.01)	0.28(0.05)	0.25(0.03)
R_q (µm)	0.13(0.03)	0.19(0.02)	0.40(0.08)	0.37(0.06)
R_z (µm)	0.96(0.14)	1.50(0.21)	2.62(0.56)	2.19(0.35)

The thermal desorption mass spectrometry (TDS) apparatus developed at CNAM [13], [14] was used to identify the surface contaminants on the test discs and their rate of desorption when heated under vacuum. This apparatus causes the desorption of physisorbed molecules on a surface by heating it from ambient temperature up to a maximum of 1275 K whilst in a vacuum of about 10^{-6} Pa. Temperature programmed desorption (TPD) [15], [16] was selected as the best method for analysing the surface contamination. The TDS apparatus is shown in figure 24 and is composed of three main parts: an analysis chamber with a high resolution quadruple mass spectrometer (Pfeiffer QMA 400 with a QMS 422 controller and a QMH 410 frequency generator), a glove-box to transfer the sample stored under inert gas, and a load-lock system to transfer the sample from the glove-box to the vacuum chamber.

6.2 Measurement procedure

The four discs were cleaned using the same procedure as described for the NPL test artefacts (§ 4.1) and were then stored in laboratory air at a nominal temperature of 20 °C and 50 % RH for one week to allow the discs to stabilise. The first disc was then transferred to the analysis chamber via the glove box and load lock chamber which were filled with dry nitrogen gas. Nitrogen N60 gas (Air Liquide, France) was used with the following specified relative amounts of contaminants; $H_2O < 0.6 \times 10^{-6}$, $O_2 < 0.1 \times 10^{-6}$, $CO_2 < 0.05 \times 10^{-6}$, and $C_nH_m < 0.01 \times 10^{-6}$. TDS measurements were then performed on the first disc during the application of a constant temperature gradient of 10 $Kmin^{-1}$ up to a maximum of 375 K over a period of 3 hours. The maximum temperature was selected so that it was below the melting point of all the support materials tested. The pressure within the measurement chamber and the surface temperature of the chamber was recorded during the TDS measurements in order to calculate the rate of thermal desorption. Mass spectra between 1 and 128 atomic units (au) were also recorded.

The disc was then transferred through the glove box filled with nitrogen gas into a storage vessel containing nitrogen gas. After a period of 1 week the disc was transferred back into the TDS measurement chamber and the measurement procedure described above was repeated.

The disc was again transferred through the glove box to storage under a bell jar in ambient air at 50 % RH. After a period of 1 week the disc was transferred back into the TDS measurement chamber and the measurement procedure repeated. This entire measurement process was then repeated for all of the discs made from the different support materials.

6.3 Results

The measured desorption rate of all desorbing molecules for each support material is shown in figure 25. The disc manufactured from Torlon was the most desorbing material followed by PEEK, with PTFE being the least desorbing material. The maximum amplitude of desorption corresponded to a surface temperature of about 350 K and no desorption was observed at temperatures below 300 K.

The surface coverage, proportional to the quantity of desorbed contamination, was measured in the TDS apparatus for each of the support materials tested and the results are shown in figure

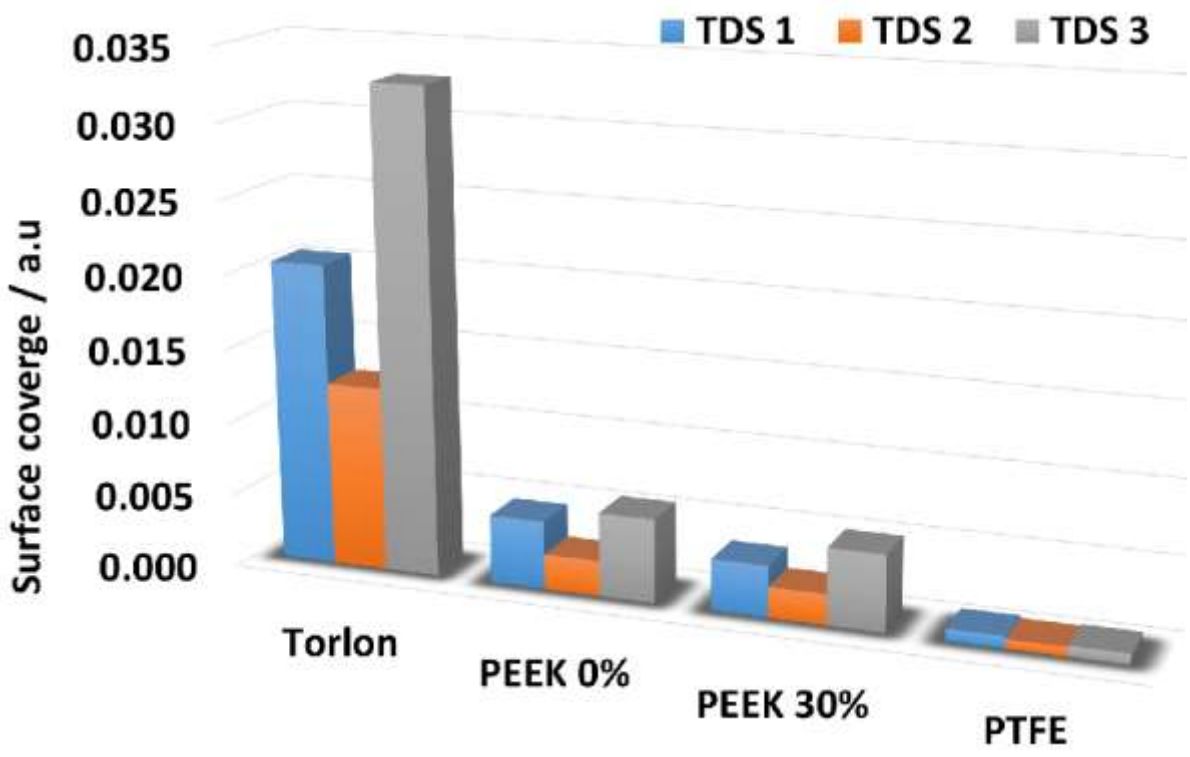

Figure 2626. Again the Torlon support material showed the highest amount of contaminants on the surface compared with the PEEK and PTFE materials. The results also showed that the TDS2 measurements that were made after storage in nitrogen gave the lowest readings for all

three materials which demonstrated that storage in nitrogen caused less contamination to form on the surface of the discs compared with storage in air.

The amounts of water, nitrogen, oxygen and carbon dioxide molecules desorbed from the surface of the discs are shown in figure

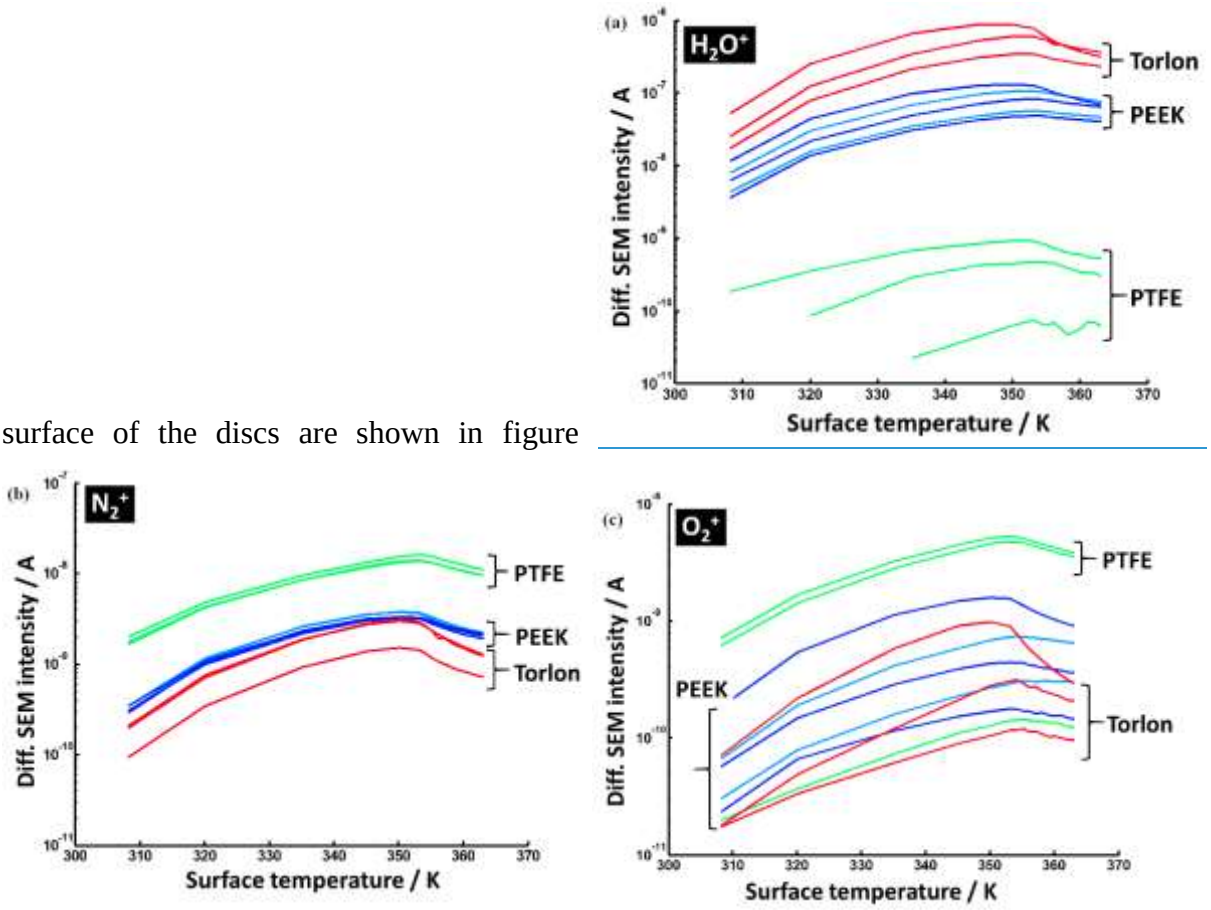

Figure 2727. Analysis of the mass spectra for all the support materials showed that water was the main component desorbed from the surface. Water and carbon dioxide were the main molecules desorbed from Torlon and PEEK. The PTFE disc desorbed much less water compared with the other discs and desorption of nitrogen and oxygen molecules were higher for PTFE.

The surface coverage amounts of water, nitrogen, oxygen and carbon dioxide molecules measured on the support materials is shown in figure 28. Water molecules are the main contaminant on the surface of the air stored samples though their quantity was reduced by the use of nitrogen as a storage medium. The results show that nitrogen was absorbed more on PTFE compared with the other materials and carbon dioxide was absorbed more on Torlon. However, the quantities of nitrogen and carbon dioxide measured were very small amounts.

7 Discussion

7.1 Thermal desorption properties

Desorption from the surface of four support materials (PEEK 0 % carbon, PEEK 30 % carbon, PTFE and Torlon grade 4435) was measured as the surfaces were heated in vacuum. The mass spectrometer did not detect desorption of water molecules from the surface of the materials until the temperature was increased above 300 K. At temperatures above 300 K a greater amount of water molecules were desorbed from the Torlon material compared with PEEK and PTFE. The rate of desorption of water molecules was also greater for the Torlon material compared with the other materials. Therefore in terms of water desorption Torlon was a less suitable material for use in a vacuum environment compared with either PEEK or PTFE.

7.2 Support test measurements

Repeated contact tests were made between stainless steel artefacts and support pegs made from PEEK, aluminium, PTFE, Torlon, and titanium. All the studied materials caused marks to appear on the surfaces of the stainless steel artefacts. Repeated contact with PEEK, aluminum, Torlon and titanium caused indentations on the surface of the artefacts. The tests at NPL with PTFE pegs also resulted in indentations on the stainless steel surface. This contrasted with the tests at MIKES where no indentations were found but contamination, presumably transferred from the PTFE pegs, was observed on the stainless steel surface. The indentations caused by contact with pegs manufactured from the polymer materials were likely to have been caused by a high yield strength contaminant embedded on the surface of the pegs. In the case of the PTFE tests at MIKES the pegs may not have accrued any contaminants during the tests.

Contact with titanium caused only shallow indentations, with a depth of about 30 nm, and some surface contamination. This result was surprising as the titanium material had similar yield strength to the aluminium material and it might be expected that pegs manufactured from these materials would results in similar damage to the stainless steel surfaces. It seems that aside from the hardness of the contact material, also the surface roughness, *i.e.* shape and size of asperities, might have a significant influence on the degree of surface damage.

These results indicate that despite titanium having a high yield strength and hardness compared with polymer materials it may be a more suitable material for use in the handling mechanism of a mass comparator or watt balance as it has caused the least amount of damage to the artefact's surface and did not transfer a significant amount of material to the artefact.

In terms of a material for use in storage vessels PEEK, aluminum, Torlon and titanium may be considered suitable as contact materials for primary mass standards, because contact with these materials does not appear to transfer significant levels of contamination to the surface. However, these materials also leave marks on the surface and thus alter the surface topography. Surface defects such as scratches are known to be preferential sites for adsorption of contaminants [17] and therefore indentations may have an effect on the surface adsorption behavior and subsequent long term mass stability of mass standards. PTFE appeared to have caused much less damage to the surface of the artefacts although the MIKES results showed significant build up in contamination. This buildup of PTFE contamination through repeated contact may not be a problem for its use in storage vessels as the artefacts may be continually stored for periods of months or even years. Assuming the amount of contamination transferred upon each contact is very small then over long time periods mass gain due to transfer of contamination might be negligible.

8 Conclusion

An evaluation of PEEK, aluminium, PTFE, Torlon and titanium materials for use in supporting mass standards in vacuum / inert gas has been undertaken. Tests that repeatedly contacted the materials with stainless steel artefacts showed that all the materials caused marks on the surface of the artefacts. Support pegs made from PEEK, aluminium, Torlon and titanium caused damage on the surface in the form of indentations and / or grooves. Out of these four materials

the titanium pegs caused the least amount of damage with smaller and shallower indentations compared with the other materials.

The MIKES results showed that the support pegs made from PTFE caused less damage compared with the other materials but also showed evidence of contamination forming on the surface, presumably due to transfer of PTFE material from the pegs. However, the NPL work showed that the PTFE pegs caused a similar amount of damage as the other polymer materials. It is possible that the PTFE pegs used by MIKES did not attract particulate contamination and hence did not damage the surface.

PEEK, PTFE and Torlon materials were also assessed with regard to their thermal sorption properties in vacuum. The molecular desorption rate for Torlon was much higher than PEEK and PTFE particularly with regard to water desorption. Therefore with respect to desorption in vacuum PEEK and PTFE are more suitable materials to manufacture supports for artefacts compared with Torlon.

In terms of selecting a suitable material for use in the weight handling mechanism in a mass comparator or watt balance titanium appears to be the most suitable material as it caused the least amount of damage and did not transfer significant amounts of material to the surface of the artefacts. Selecting a suitable material for use in an inert gas storage device depends on whether reducing damage to the surface of an artefact is a more critical variable, in which case PTFE or titanium would be the most suitable materials, or whether reducing the transfer of contamination to the artefact is more important in which case PEEK, aluminium or titanium were more suitable. Further research is required to determine whether surface damage or material transfer contamination is the critical component affecting the mass stability of artefacts before a decision can be made on the best material to use for supporting mass standards in vacuum / inert gas. Also, examining the topography and chemical identification of the surface of the pegs before and after the contact tests would confirm whether there is contamination present and its composition.

ACKNOWLEDGEMENTS

The authors acknowledge the financial support of the National Measurement Systems Directorate of the UK National Measurement Office.

This work is part of the EURAMET Joint Research Project SIB05 NewKILO. It received funding from the European Union's Seventh Framework Programme, ERANET Plus, under grant agreement 217257.

Figure 1 Modified turntable of the HK1000 mass comparator fitted with the test pegs manufactured from the support materials.

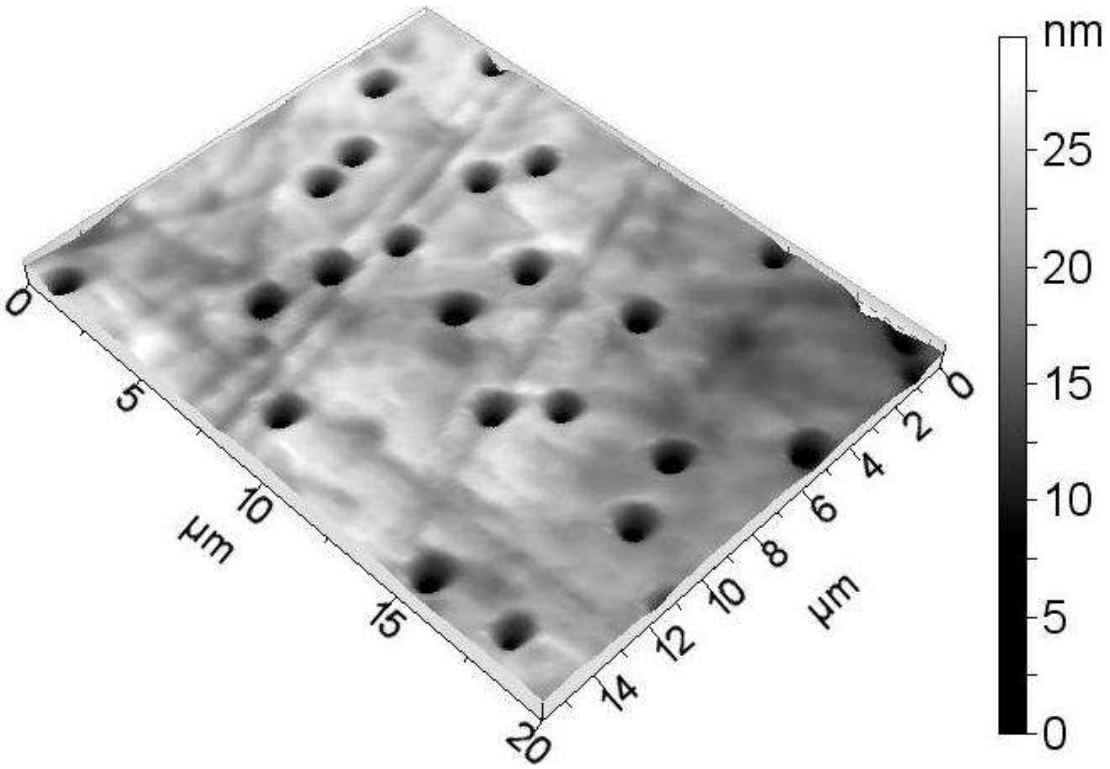

Figure 2. An isometric plot of a CSI image (the z-scale has been magnified by 5%) of the indenations caused by an aluminium peg.

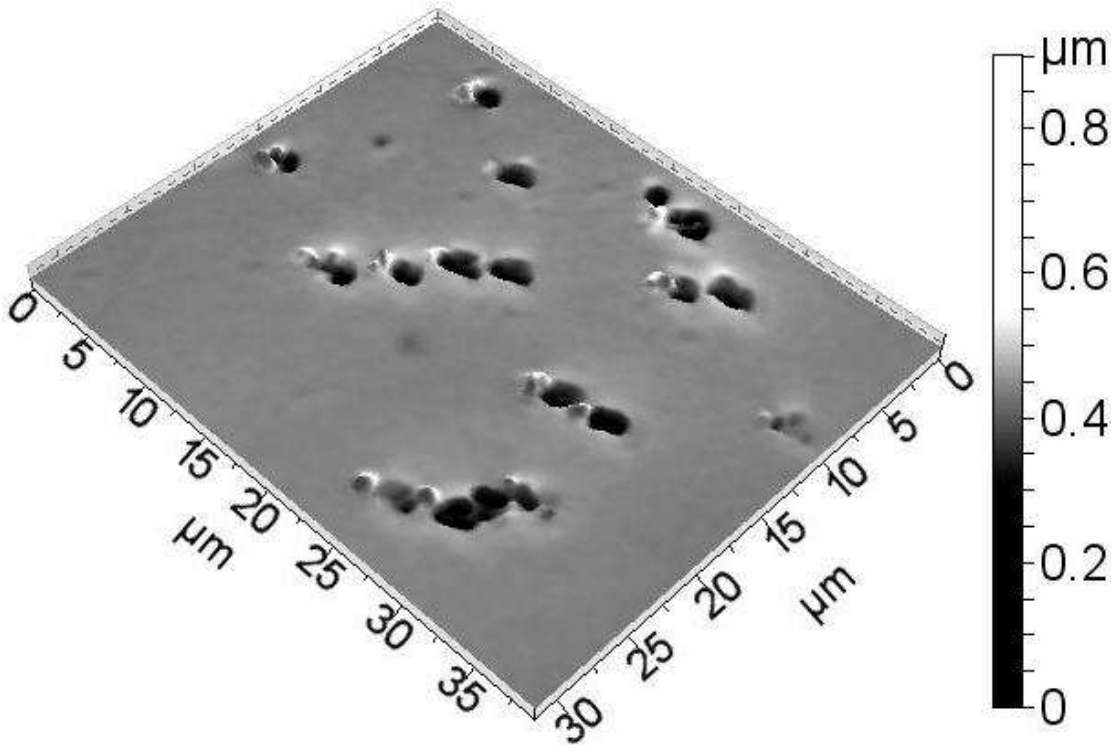

Figure 3. CSI image showing indentations that appear elongated and have a build-up of material (z-scale magnified by 5%).

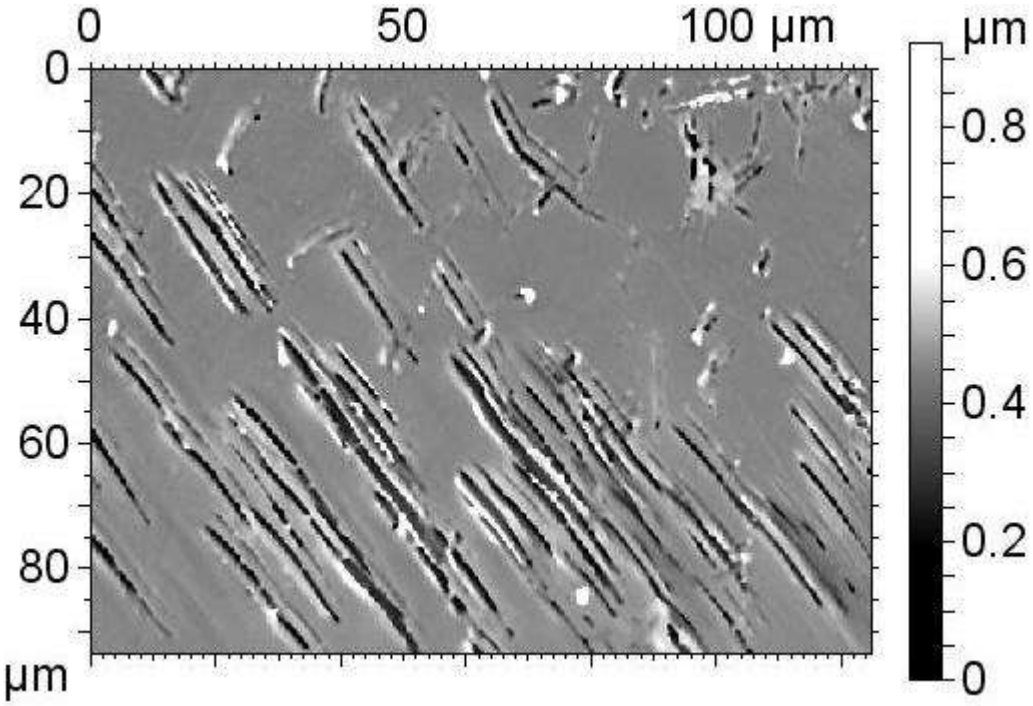

Figure 4. CSI images showing groove damage resulting from sliding contact with an aluimium peg.

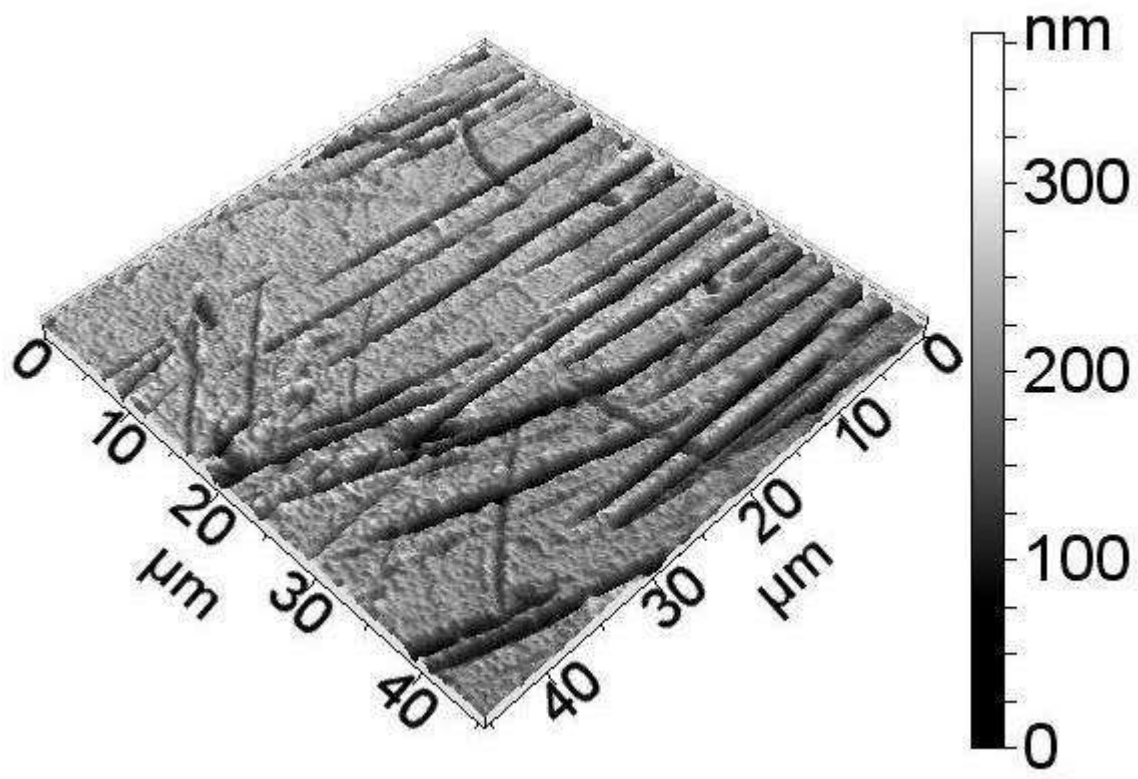

Figure 5. The AFM image shows the depths of the grooves to be around 300 nm.

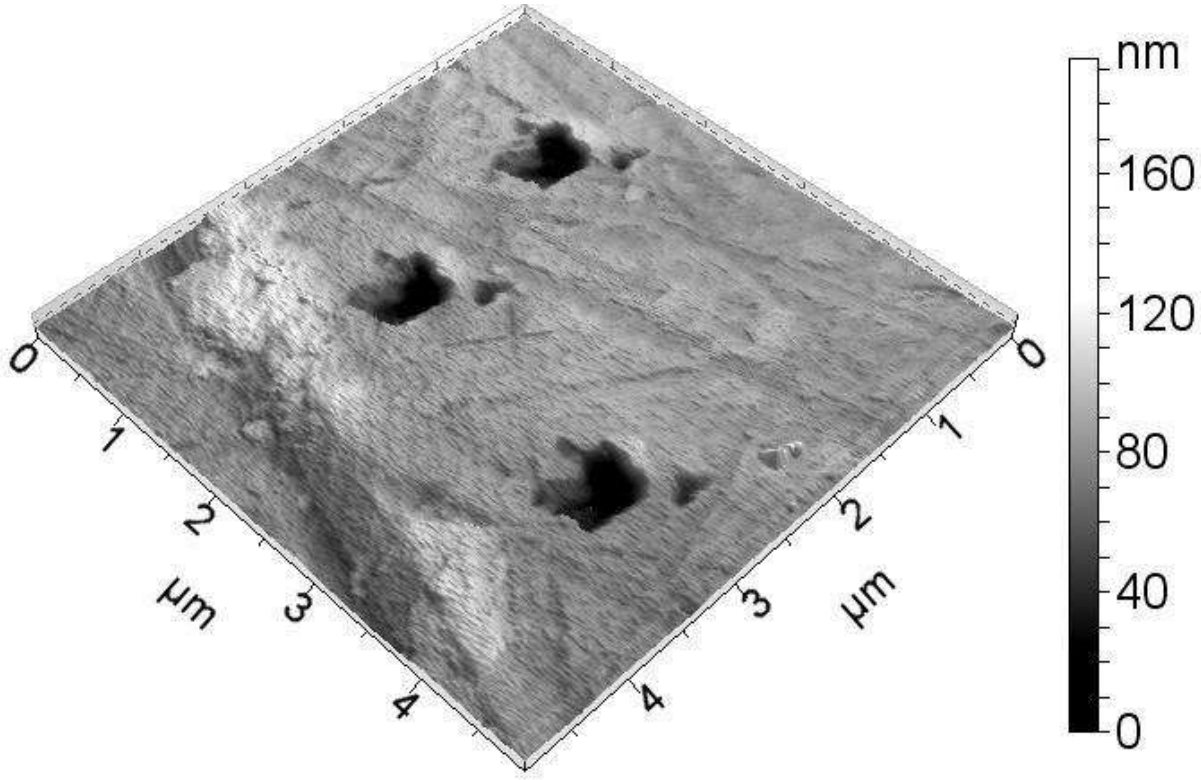

Figure 6 Indentations measured with non-contact mode AFM; the improved lateral resolution reveals their irregular shape. The depth of the indentations is around 100 nm.

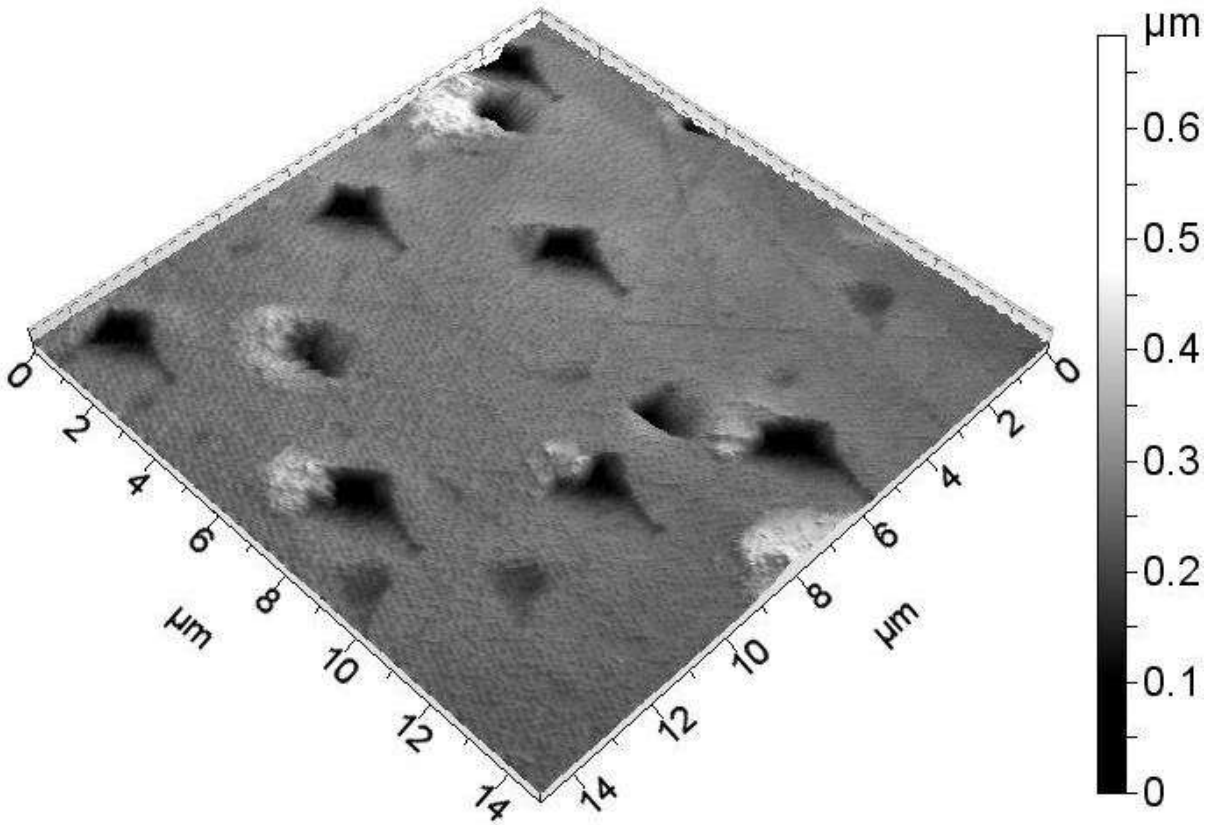

Figure 7 AFM image of a region that has indentations with a build-up of material.

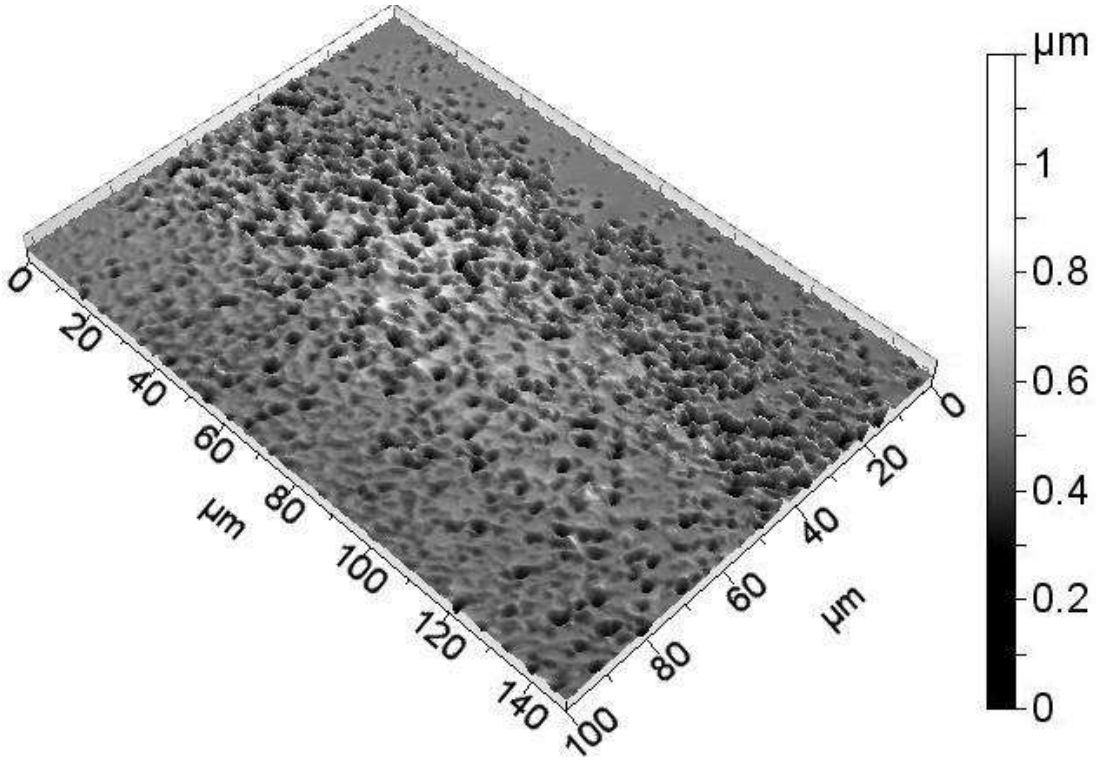

Figure 8. CSI image showing the damage accrued after multiple contacts with an aluminium peg over a small area.

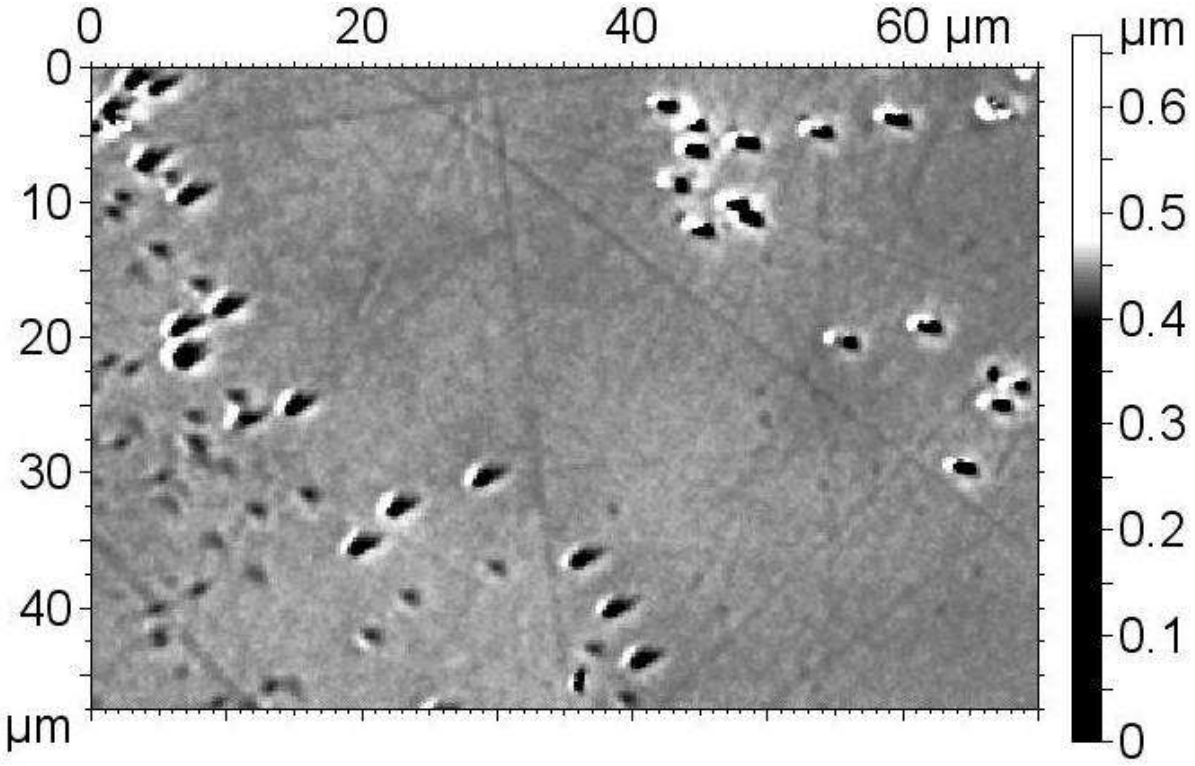

Figure 9. CSI image showing **i**ndentations that have resulted from contact with a PEEK peg.

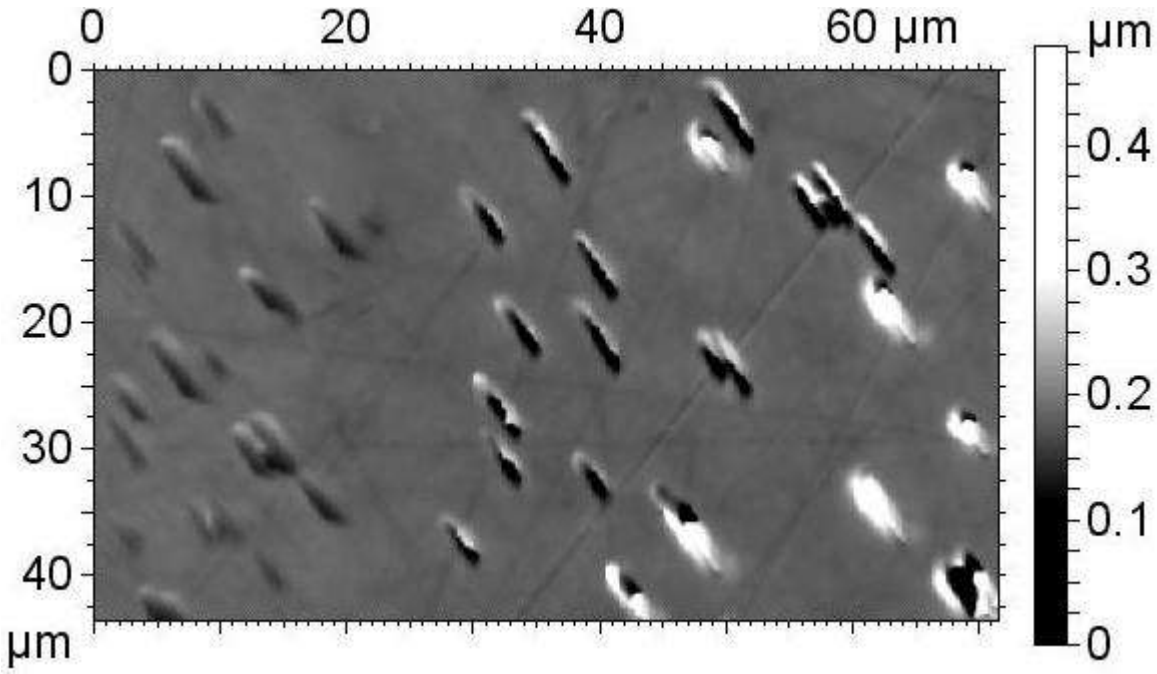

Figure 10. CSI image of the grooves caused by sliding contact with a PEEK peg.

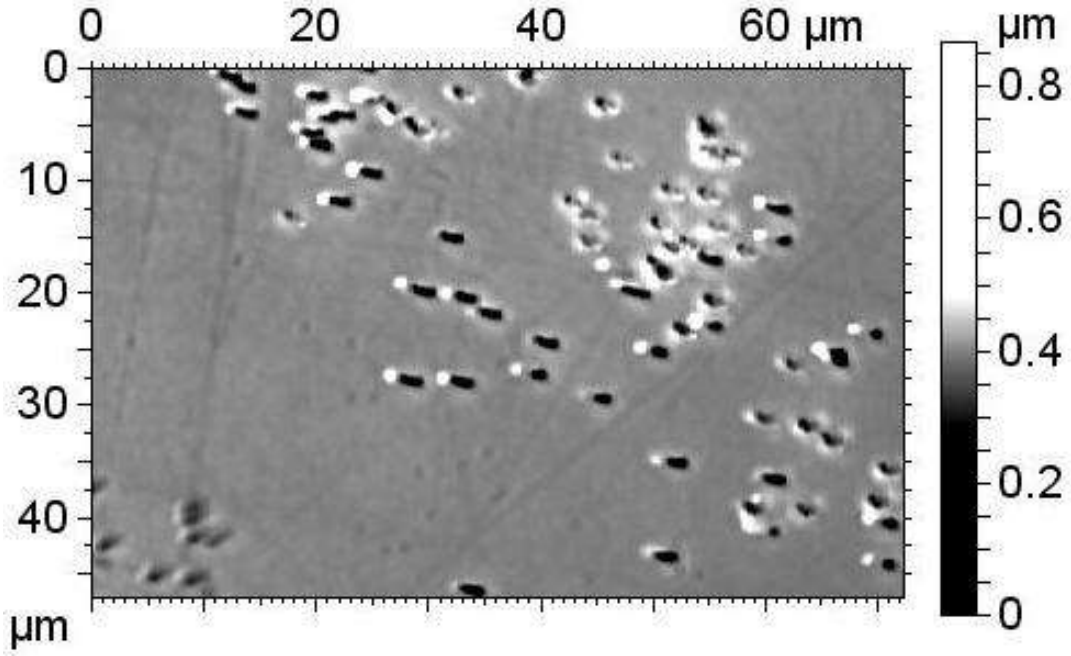

Figure 11. CSI image of the indentations resulting from repeated contact with a PTFE peg.

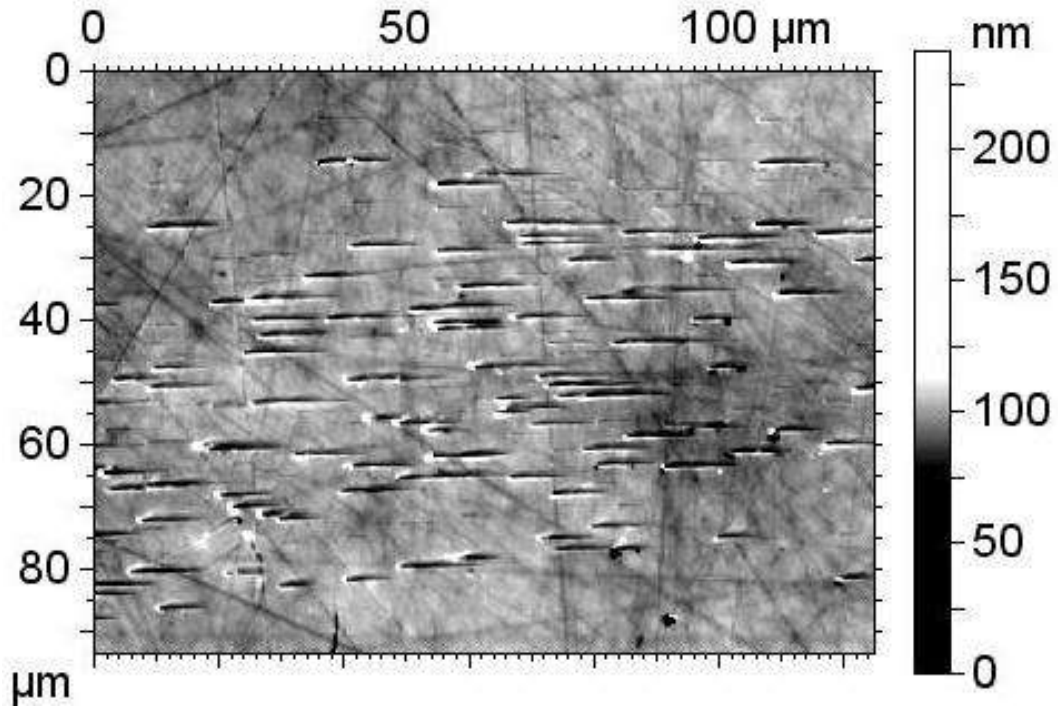

Figure 12. CSI image of the grooves caused by sliding contact with a PTFE peg.

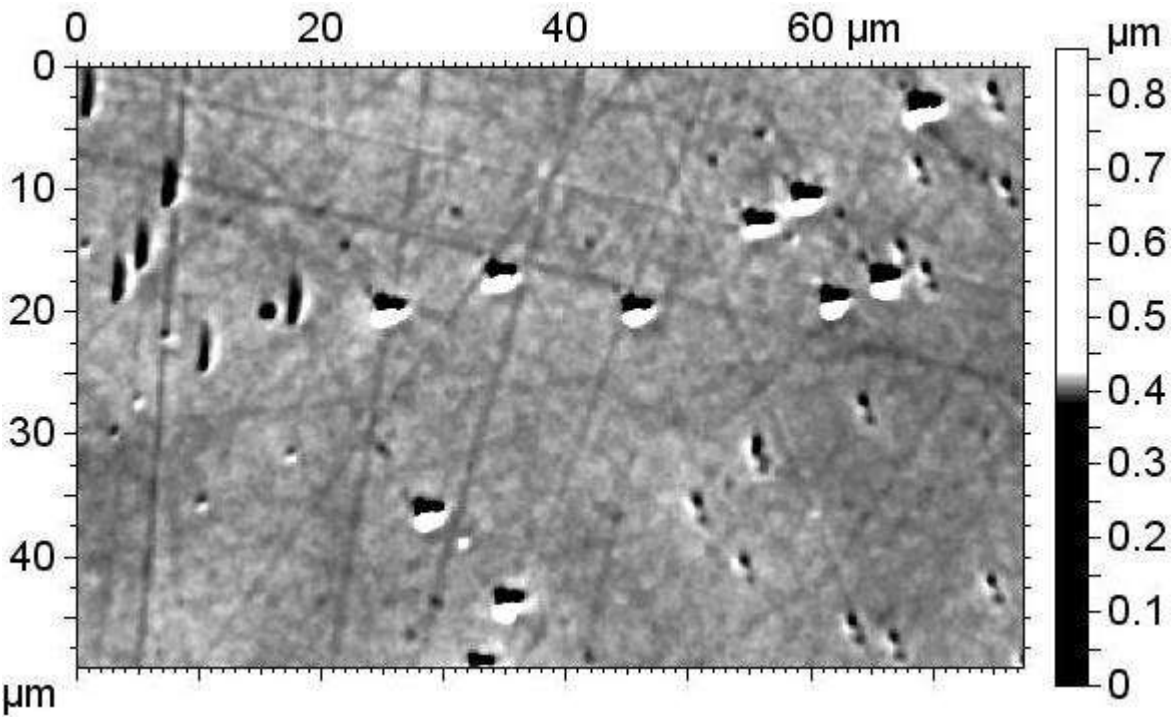

Figure 13. CSI image of the indentations resulting from repeated contact with a Torlon peg.

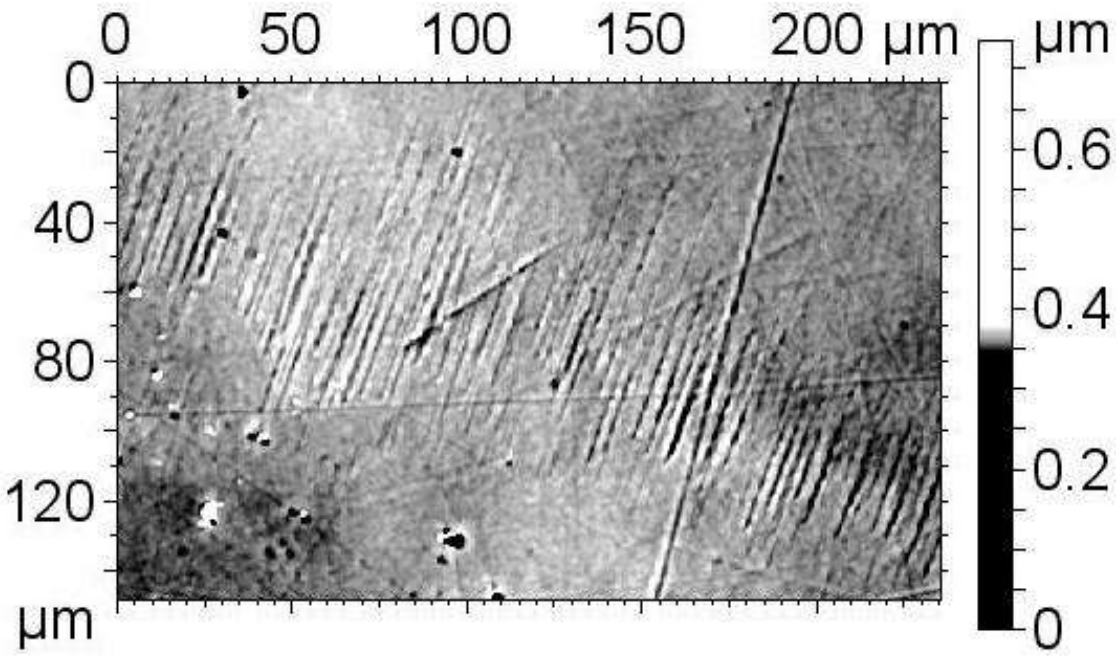

Figure 14. CSI image of the grooves caused by sliding contact with a Torlon peg.

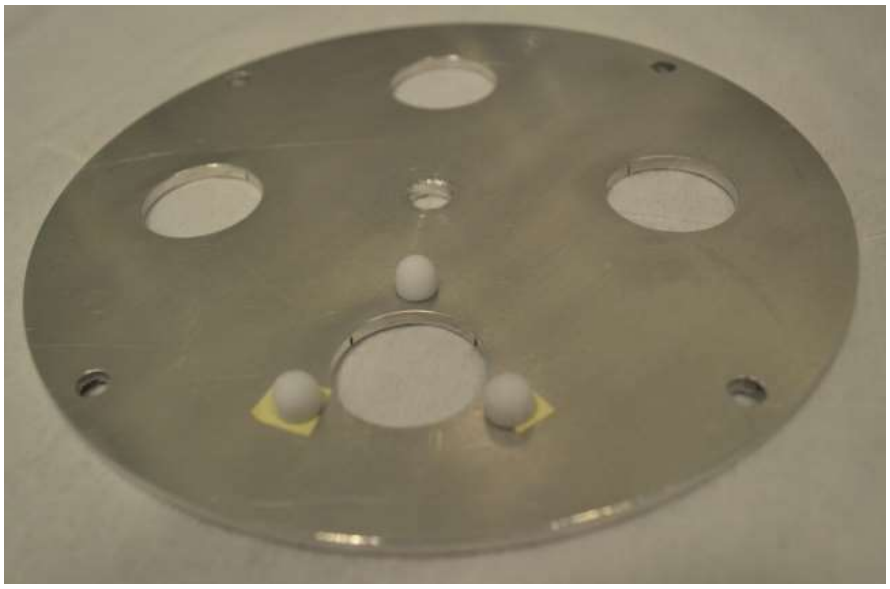

Figure 15. PTFE pegs attached to the comparator turntable.

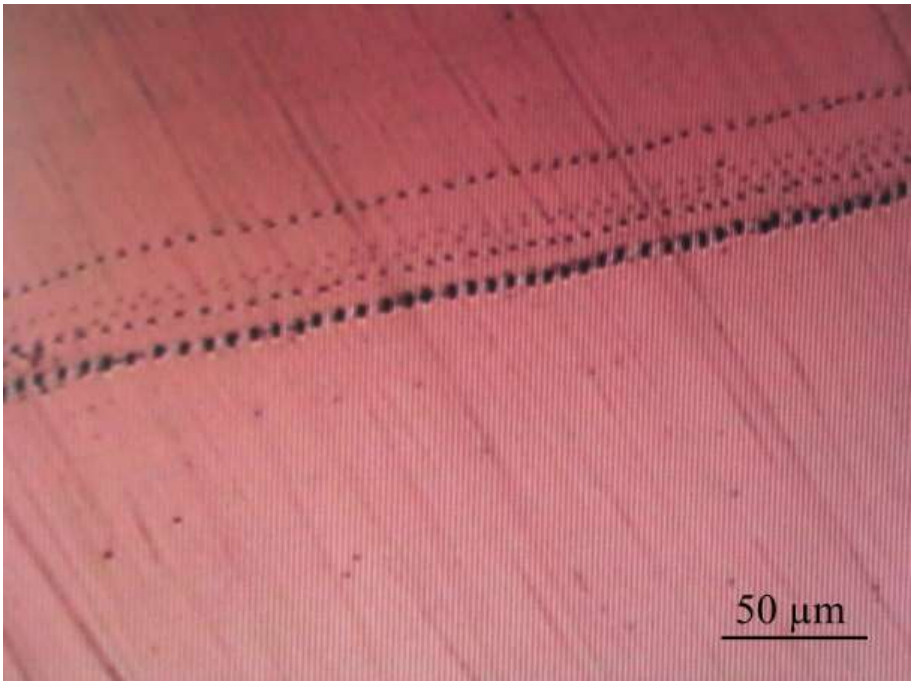

Figure 16. Optical microscope image of the contact area for PEEK.

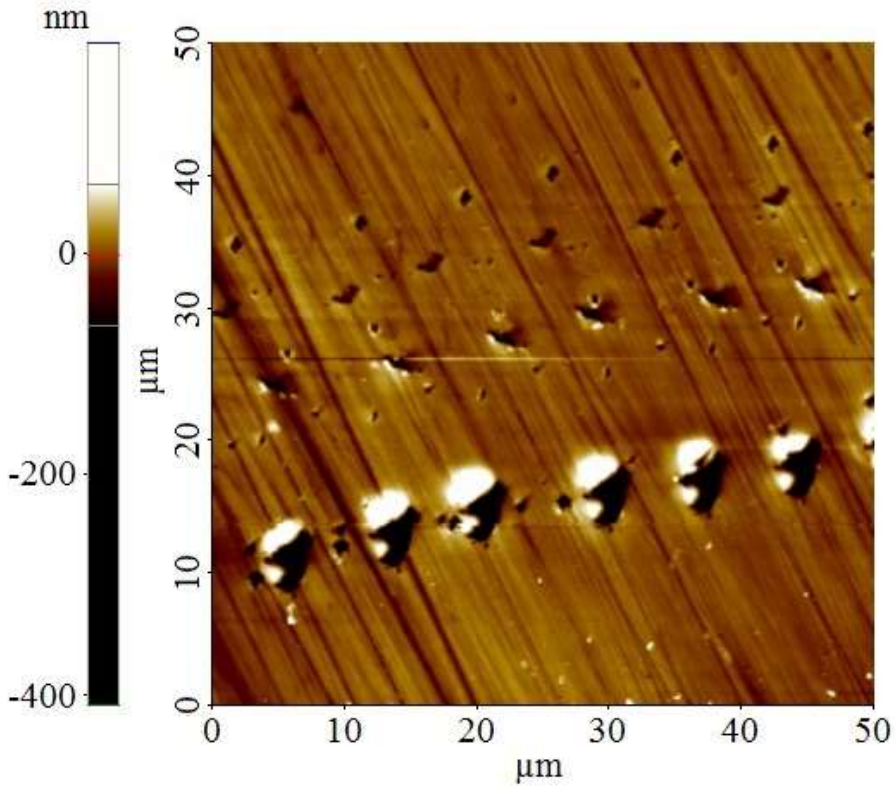

Figure 17. AFM topography image of the contact area for PEEK.

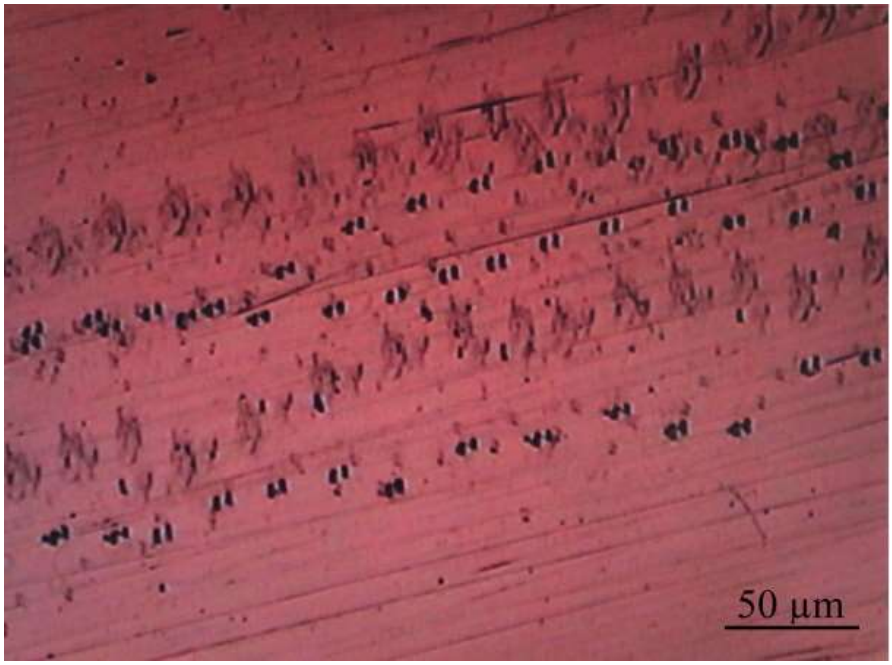

Figure 18. Optical microscope image of the contact area for aluminium.

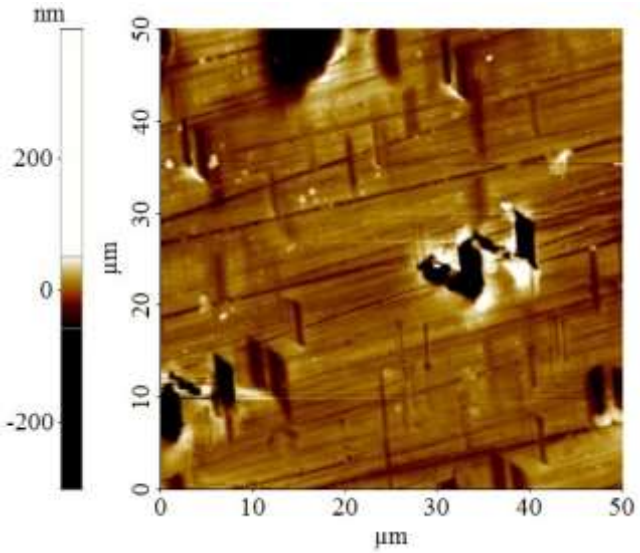

Figure 19. AFM topography image of the contact area for aluminium.

Figure 20. Optical microscope image of the contact area for PTFE.

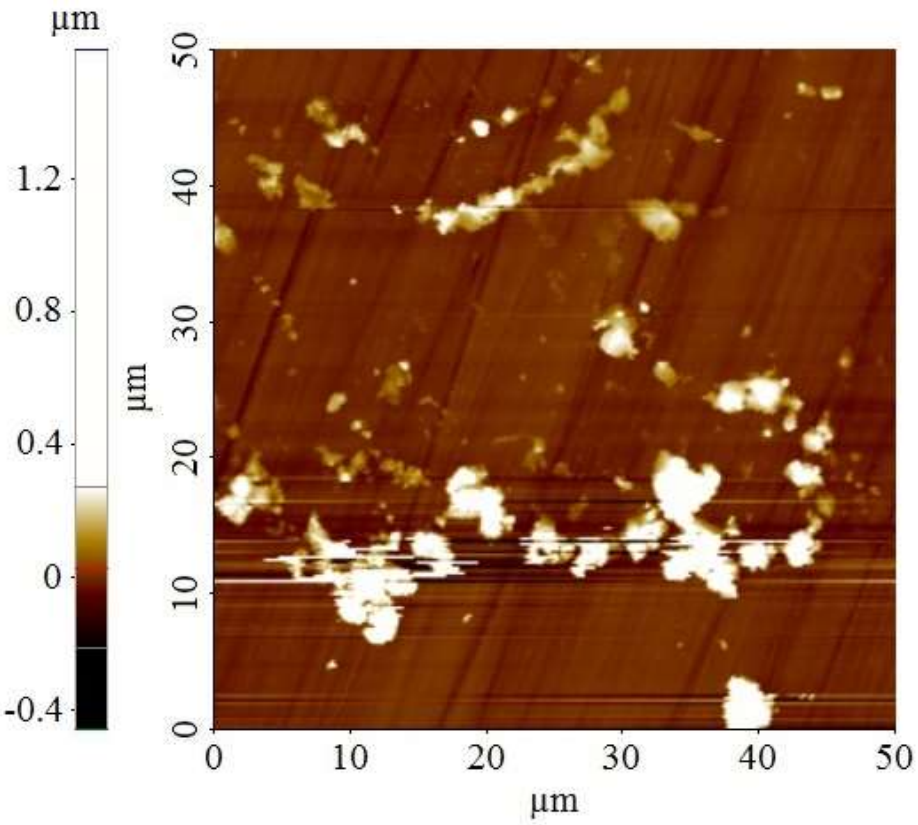

Figure 21. AFM topography image of the contact area for PTFE.

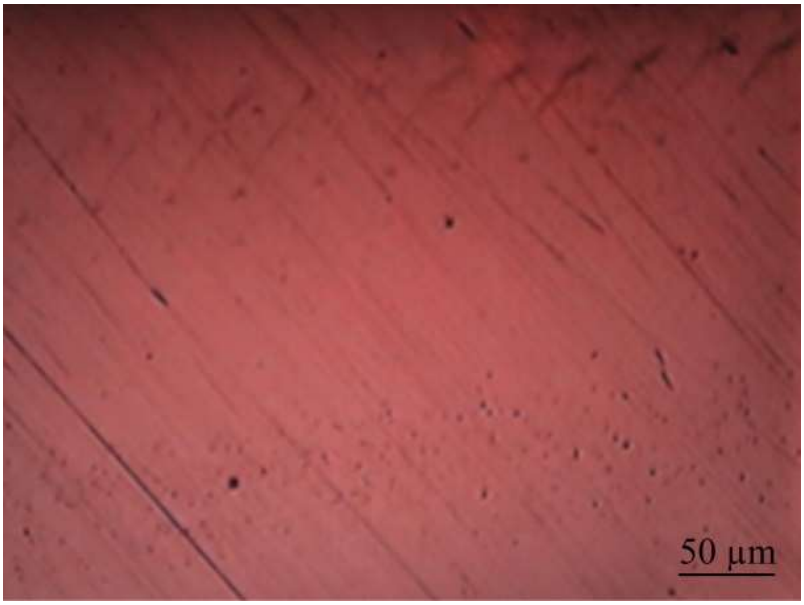

Figure 22. Optical microscope image of the contact area for titanium.

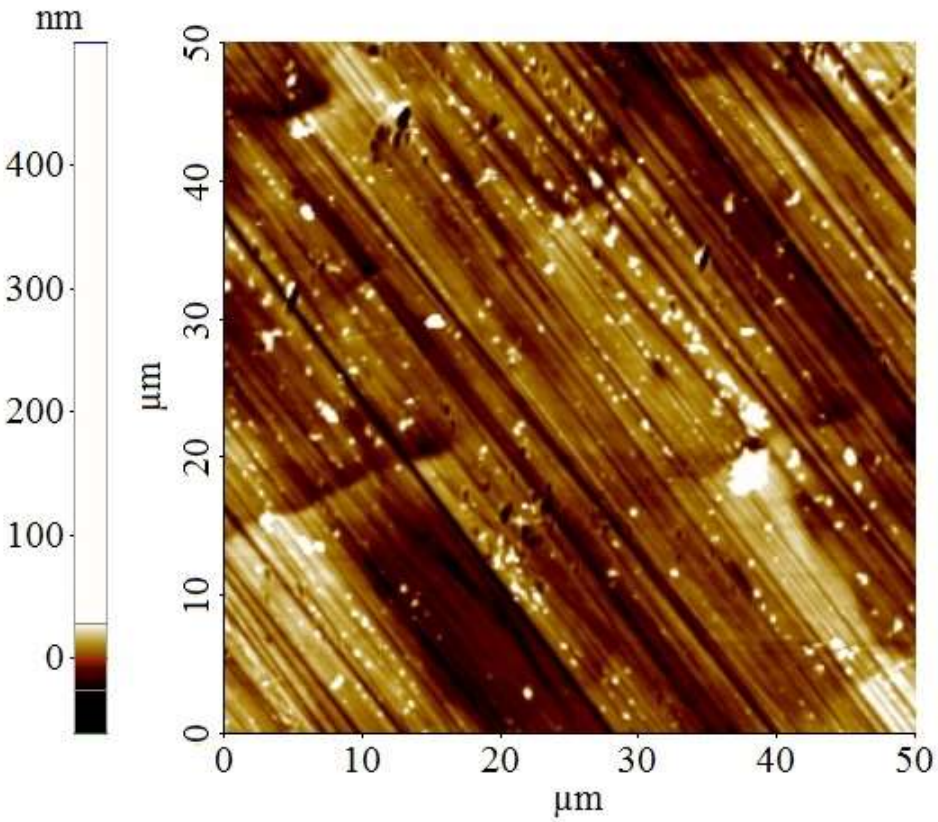

Figure 23. AFM topography image of the contact area for titanium.

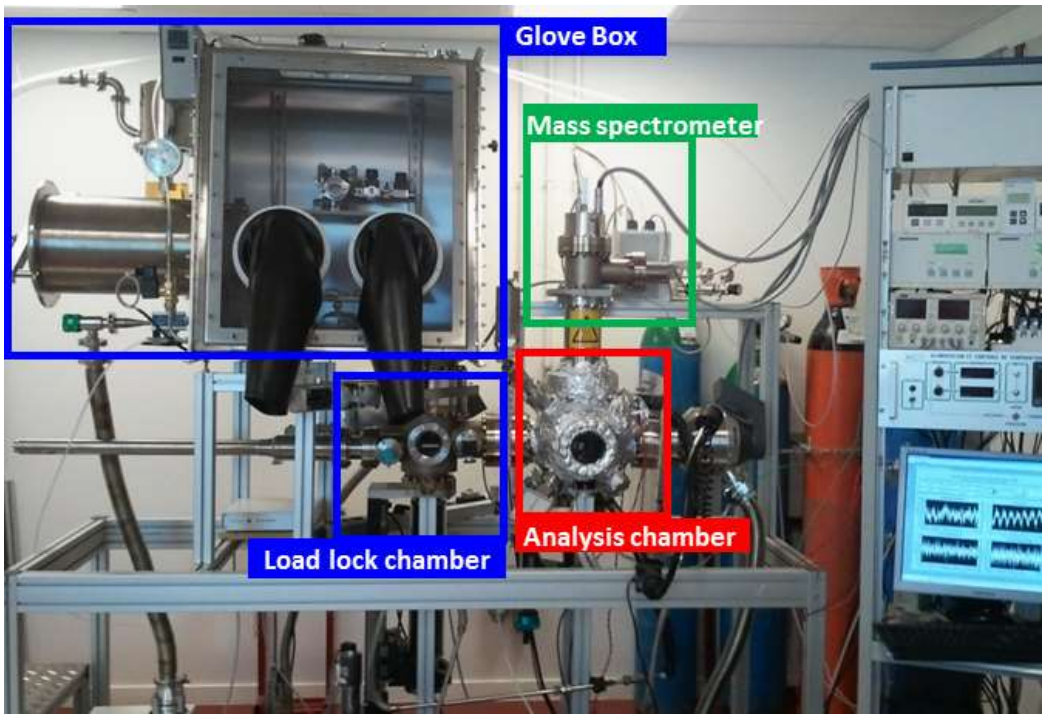

Figure 24. Photograph of the TDS apparatus.

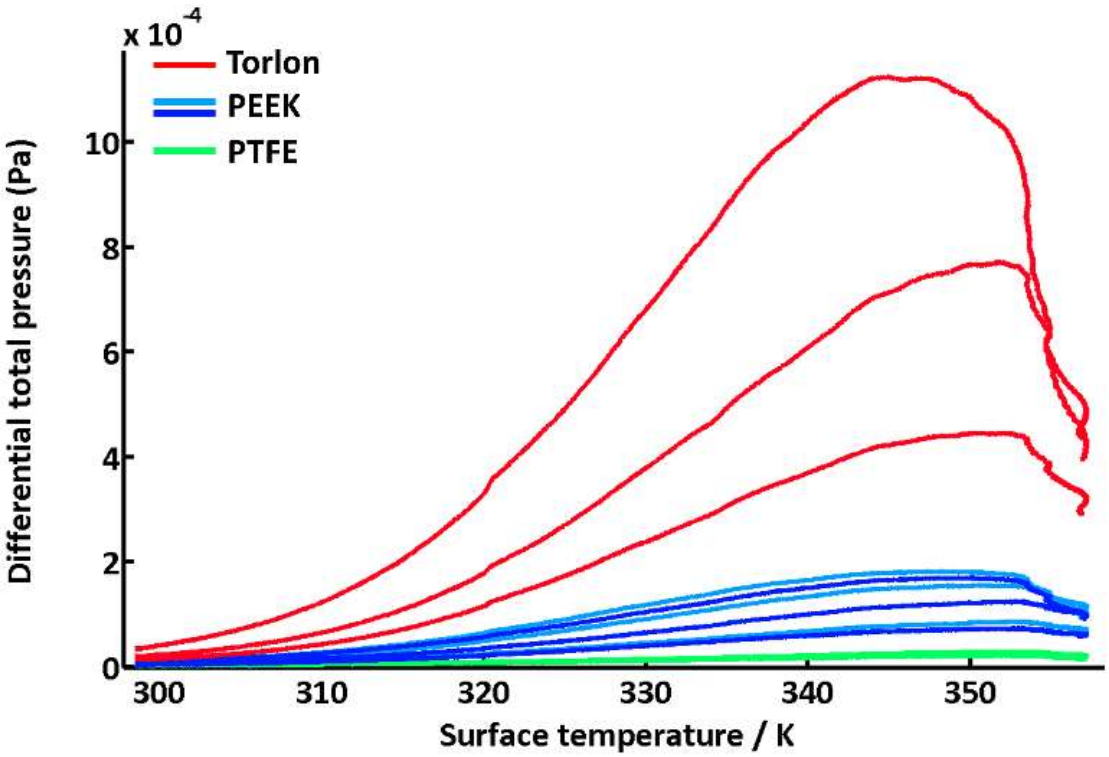

Figure 25. Desorption rate curves for each contact material and for each thermal desorption. Red lines for Torlon, blue lines for PEEK and green lines for PTFE.

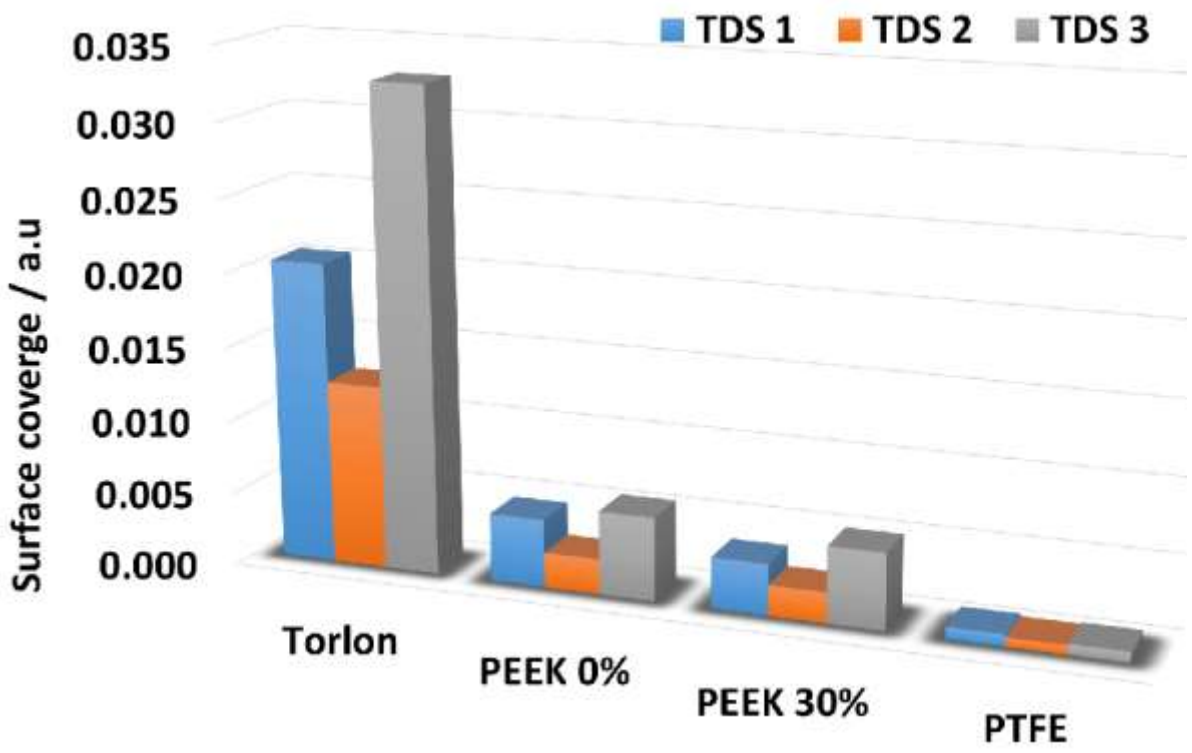

Figure 26. Surface coverage for each thermal desorption and each contact material. TDS1 was after initial cleaning, TDS2 was after 1 week in dry nitrogen gas, and TDS3 was after 1 week storage in air.

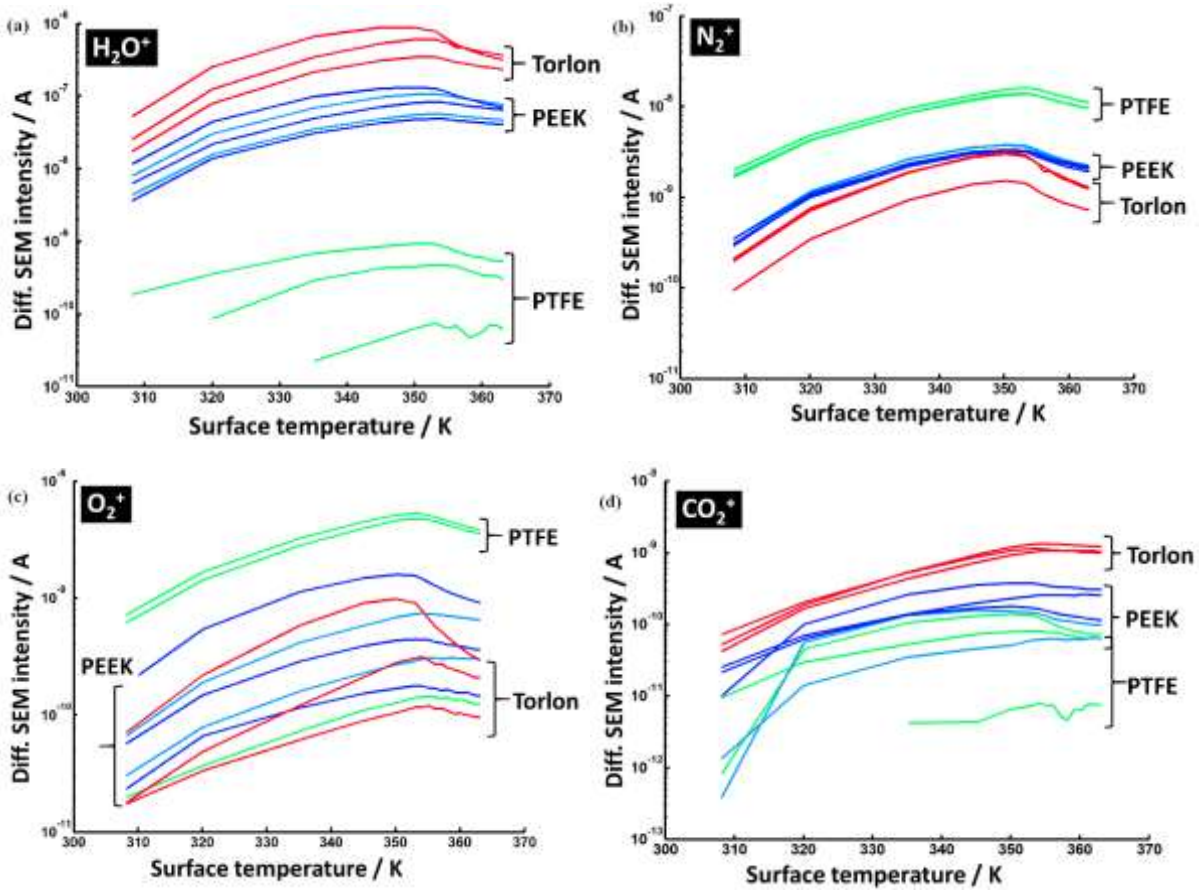

Figure 27. Molecular desorption rate curves for each support material and for each thermal desorption measurement. Red lines for Torlon, blue lines for PEEK and green lines for PTFE. (a) H_2O, (b) N_2, (c) O_2 and (d) CO_2.

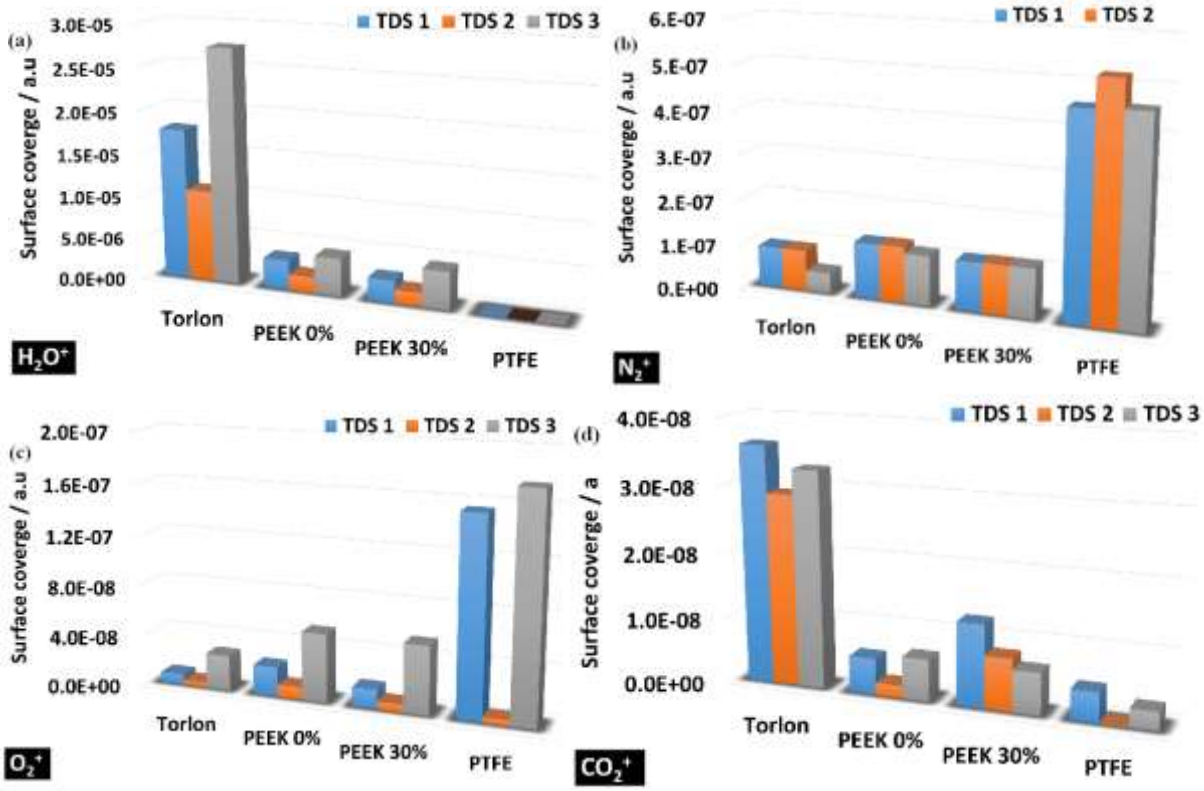

Figure 28. Surface coverage for each thermal desorption and each support material. TDS1 after initial cleaning, TDS2 after 1 week storage in nitrogen and TDS3 after one week storage in air at 50 % RH. (a) H_2O, (b) N_2, (c) O_2 and (d) CO_2.

References

[1] Davis R 2003 The SI unit of mass *Metrologia* **40** 299-305

[2] Stock M 2013 Watt balance experiments for the determination of the Planck constant and the redefinition of the kilogram *Metrologia* **50** R1-R16

[3] Becker P, Friedrich H, Fujii K, Giardini W, Mana G, Picard P, Pohl H-J, Riemann H and Valkiers S 2009 The Avogadro constant determination via enriched silicon-28 *Meas. Sci. Technol.* **20** 092002

[4] Euromet 509

[5] Barat P, Berry J, Borys M, Davidson S, Fehling T, Fuchs P, Malengo A, Meury PA and Silvestri Z 2013 Report detailing requirements of NMIs for storage and transfer equipment compatible with existing apparatus *National Physical Laboratory Report* ENG 43

[6] Fen K and Morris E C 2008 An experimental study of the stability of mass standards in transit *Metrologia* **45** 233-240

[7] Davidson S 2012 Characterization of the long-term stability of mass standards stored in vacuum by weighing and surface analysis *Metrologia* **49** 200-208

[8] Fuchs P, Marti K and Russi S 2012 Materials for mass standards: long-term stability of PtIr and Au after hydrogen and oxygen low-pressure plasma cleaning *Metrologia* **49** 615-627

[9] Berry J, Davidson S 2011 Evaluation of equipment and procedures for the transfer and storage of mass standards in inert gas *Metrologia* **48** 391-398

[10] OIML R 111-1 2004 Organisation Internationale de Métrologie Légale

[11] Giusca C and Leach R 2013 Calibration of the scales of areal surface topography measuring instruments: part 3. Resolution *Meas. Sci. Technol.* **24** 105010

[12] de Groot P and Colonna de Lega X 2006 Interpreting interferometric height measurements using the instrument transfer function *Proc. FRINGE 2005* 30–7

[13] Silvestri Z and Pinot P 2009 Thermal Desorption mass Spectrometry (TDS). Application on mass metrology *XIX IMEKO World Congress Fundamental and Applied Metrology (Lisbon, Portugal, 2009)*

[14] Silvestri Z, du Colombier D, Macé S, and Pinot P 2011 Moyens de caractérisation des surfaces et leurs applications en métrologie *Rev. Fr. Métrologie* **48** 11‑20

[15] Holmes Parker D, Jones M E, and Koel B E, 1990 Determination of the reaction order and activation energy for desorption kinetics using TPD spectra: Application to D2 desorption from Ag(111) *Surf. Sci.* **233** nº 1‑2 65‑73

[16] Rudzinski W, Borowiecki T, Panczyk T and Dominko A 2000 A quantitative approach to calculating the energetic heterogeneity of solid surfaces from an analysis of TPD peaks: comparison of the results obtained using the Absolute Rate Theory and the Statistical Theory of Interfacial Transport, *Thermochim. Acta*, **104** n^{o} 9 1984–1997

[17] Högström R, Korpelainen V, Riski K, and Heinonen M 2010 Atomic force microscopy studies of surface contamination on stainless steel weights. *Metrologia* **47** 670